CHINESE OPTICS LETTERS

Vol. 21, No. 3 | March 2023

Method for active spatial alignment and stabilization of laser beams in multi-beam systems

Chenliang Ding (丁晨良)[1,2], Dazhao Zhu (朱大钊)[1,2], Chengpeng Ma (马程鹏)[1], Mengbo Tang (汤孟博)[1], Zhenyao Yang (杨臻垚)[1], Yong Liu (刘 勇)[1,3], Cuifang Kuang (匡翠方)[1,2*], and Xu Liu (刘 旭)[1,2]

[1] Research Center for Intelligent Chips and Devices, Zhejiang Lab, Hangzhou 311121, China

[2] State Key Laboratory of Modern Optical Instrumentation, Department of Optical Engineering, Zhejiang University, Hangzhou 310027, China

[3] College of Electronics and Information Engineering, Shanghai University of Electric Power, Shanghai 200090, China

*Corresponding author: cfkuang@zju.edu.cn

Received June 17, 2022 | Accepted November 11, 2022 | Posted Online February 24, 2023

We propose a new method for the development of multi-beam systems for the spatial alignment and stability of beams based on the error separation technique. This method avoids alignment errors caused by coupling effect of piezoelectric devices, inaccurate correction calculations, and detection mode of the angular deviation. According to the results by external detectors, the error value of spatial alignment and the root mean square (RMS) of deviations under control during 1 h can be equivalent to approximately 0.87 and 1.06 nm at the sample plane under an oil immersion lens (focal length $f = 2$ mm). The RMS of deviations is less than one-third of those currently reported for multi-beam systems; therefore, higher alignment and stability accuracy can be achieved with our proposed method.

Key words: beam stabilization; multi-beam microscopy; high-precision correction; decoupling.

DOI: 10.3788/COL202321.031201

1. Introduction

The interaction between the laser and the material is an effective way to break the diffraction limit, both for super-resolution imaging and lithography. With the development of stimulated emission depletion (STED)[1], resolution augmentation through photo-induced deactivation (RAPID) lithography[2], two-color photo-initiation/inhibition (2PII) lithography[3–5], and other theories, multi-beam systems become the inevitable trend of performance improvement. However, for these high-precision optical systems, fluctuations in the pointing of the laser beams significantly hinder further improvements in performance and applications. Therefore, the spatial alignment and stability of beams in multi-beam systems are critical for achieving the best results.

The pointing of the laser beam fluctuates along the long propagation paths from the light source to the target plane because of thermal expansion, mechanical vibrations, and spatial and temporal non-uniform nonlinear effects[6]. To minimize fluctuations, passive anti-drift is the conventional method that uses an optical platform and temperature control system. However, as the demand for precision of the system increases, the cost and technical difficulty increase significantly, making it difficult to meet the current requirements of multi-beam systems.

Different methods have been proposed to enhance beam spatial alignment and stability in various multi-beam systems. Using an optical fiber is an effective method to reduce deviations of laser beams[7] and can achieve spatial alignment by coupling two beams into the same fiber[8]. However, the dispersion effect of the optical fiber leads to pulse expansion of the femtosecond laser source, and many optical modulations still require spatial beams.

Therefore, it is highly meaningful to realize spatial alignment and stability of spatial beams. Methods based on the spatial light modulator (SLM) have been adapted to calibrate the central position of two beams in STED systems with a precision of 4.3 ± 2.3 nm[9,10]. However, these methods with SLM present difficulties in achieving real-time and high-precision stabilization. A stabilization method based on closed-loop feedback provides higher precision and faster response speed[11–13]. This approach utilizes information obtained through various detection technologies to determine appropriate corrections[14–16]. A standard deviation (STD) of approximately 1.5 μrad was achieved using a compact stabilization system in 30 min[17,18], which is equivalent to approximately 3 nm at the sample plane with a focal length of 2 mm. With the further development of multi-beam systems, higher requirements for system stability are put forward. For example, minimal photon fluxes (MINFLUXs) have attained a precision of 1 nm, resolving

molecules only 6 nm apart[19], and 9 nm feature size and 52 nm two-line resolution were achieved by three-dimensional optical beam lithography[20].

In this study, to achieve beam spatial alignment and stability automatically, we propose a new method that can be used for spatial alignment and stability of beams in multi-beam systems. The error separation technique that we previously proposed[21] was used in this method, which has the ability to avoid alignment errors caused by the coupling effect of piezoelectric devices, inaccurate correction calculations, and detection mode of angular deviation, compared with other previous calibration techniques. The spatial alignment and stability system of the double beams was built with a small size, and a pair of detectors was used to adjust the spatial alignment of the two beams, which can then exit with the same beam center and high stability. Thus, a higher alignment and stability accuracy can be achieved for further development of multi-beam systems.

2. Measurement and Alignment Principle

Figure 1(a) shows the optical system based on the error separation technique, which is described in the previous work, and the results show that the system can achieve high-precision correction and fast response with a small system size. However, the principles and advantages of this technique were not clearly analyzed in the previous work, which will be elaborated here.

The optical system consists of the control and detection units. The control unit contains a pair of fast steering mirrors (FSMs) to adjust the position and angular movements of the exit beam. The detection unit contains two detectors: one is to detect the positional deviation, and the other is to detect the angular deviation placed behind the lens. Because the focusing characteristic of the lens eliminates the influence of beam position movement, the detector can only detect the change of beam propagation angle.

This type of optical system is relatively simple, but its stability accuracy is affected by the following factors. First, the errors are caused by the coupling effect of piezoelectric devices, and an FSM with a piezo driver offers the advantages of small system dimensions, high accuracy, high bandwidth, and fast response[22,23]. However, the nonlinearity, hysteresis, and creep characteristics of piezoelectric actuators reduce the control accuracy. For the dual FSM control system, the coupling of errors will result in the failure to accurately calculate the error source, thus further reducing the control accuracy.

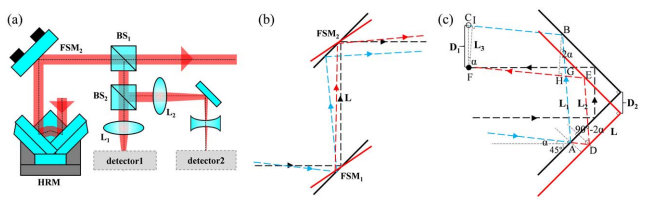

Fig. 1. (a) Optical system based on error separation technique, (b) error analysis of improved calibration optical system, and (c) error analysis of optical system based on error separation technique. FSM, fast steering mirror; HRM, hollow retroreflector mirror; BS, beam splitter; L, lens.

Second, the errors are caused by inaccurate correction calculations. The system requires the distance between the centers of the two FSMs when calculating the correction parameter values. However, when the incident beam deviates from the center of the first FSM, errors occur in the calculated correction values, which make it difficult to reach the expectation, as shown in Fig. 1(b). The black dotted line is the path of the beam under ideal conditions, the blue dotted line is the incident beam with both positional and angular beam deviations, and the red dotted line is the control result of the FSMs based on the beam deviations from detection units. It can be seen that there are errors in the feedback control.

Third, errors are caused by the detection mode of the angular deviation. The accuracy of angular detection is related to the focal length of the lens: the longer the focal length, the higher the accuracy. However, an increase in the optical path leads to an increase in instability, which results in a decrease in the detection accuracy. Therefore, it is difficult to improve the accuracy of the angle detection using ordinary lenses.

The optical structure was improved by considering the above factors. A lens was added in front of detector$_1$ to image the beam at FSM$_2$ to the test surface of detector$_1$. By introducing the object–image relationship, FSM$_1$ and detector$_1$ as well as FSM$_2$ and detector$_2$ form closed-loop systems that effectively reduce errors caused by the coupling effect of piezoelectric devices. However, it remains difficult to solve the second problem mentioned above.

The error separation technique can solve all of the problems mentioned above, and Fig. 1(c) shows the correction process using a hollow retroreflector mirror (HRM). The HRM uses three orthogonal surfaces to reflect light back to the source at the same angle as the incident beam. Unless the incident and reflected beams strike the center of the HRM, they will not overlap, but will instead be shifted with respect to each other, such that they are symmetrical about the center point where the three faces intersect. Therefore, the position of the reflected beam can be changed by shifting the HRM position. D_1 in Fig. 1(c) is the distance from the beam center to the target location on the detection surface, and D_2 is the distance that the HRM needs to move. The incident beam (blue dotted line) with positional and angular beam deviations intersects the HRM at points A and B, respectively. After reflection, it is incident to point C on the detection plane. When the HRM moves by a distance D_2 [solid red line in Fig. 1(c)], the incident laser (red dotted line) intersects the HRM at points D and E and is incident to point F on the detection plane.

According to the geometric relationship shown in Fig. 1(c), the following equations can be obtained:

$$D_1 = L_3 \cdot \cos(\alpha), \tag{1}$$

$$L_3 = (L_1 - L_2) \cdot \cos(2\alpha), \tag{2}$$

where L_3 is the distance from point F to the BC segment, and the point of intersection is I. α is the angle between the incident beam and the horizontal line, L_1 is the distance between points A and B, L_2 is the distance between points D and E, and L is the distance between point D and the center point where the three faces intersect. L_1 and L_2 are calculated using the following equations:

$$L_1 = \{L + (\sqrt{2}D_2/2)[1 + \tan(\pi/4 - \alpha)]\}/\cos(\pi/4 + \alpha), \quad (3)$$

$$L_2 = L/\cos(\pi/4 + \alpha). \quad (4)$$

By substituting Eqs. (3) and (4) into Eq. (2), the simplification is as follows:

$$L_3 = (2D_2)/\cos\,\alpha. \quad (5)$$

By substituting Eq. (5) into Eq. (1), we obtain

$$D_1 = 2D_2. \quad (6)$$

According to Eq. (6), the distance the HRM moves is always half of the deviation value detected by the detector when the incident beam has positional and angular beam deviations. Thus, after correcting the HRM, the beam can be accurately incident into the center of FSM_2, and FSM_2 can correct the angular deviation with high precision. What is more, a single lens is replaced by a group of lenses in the system, which improves the accuracy of angular deviation detection. Therefore, this optical system can solve the three problems.

3. System Configuration and Alignment Principle

According to the principle introduced, the method for spatial alignment and stability of beams in a multi-beam system is presented in Fig. 2.

It consists of two modules for the stabilization of beams of different wavelengths, and the detection part of one module can detect different wavelengths at the same time to ensure the coincidence of the intensity centers of the two beams. Figure 2(a) shows the schematic of the double beams stabilization system, and Fig. 2(b) shows the experimental setup. Wavelengths of 780 and 532 nm were used in the system, which is consistent with that used in super-resolution imaging or super-resolution lithography.

The first laser beam ($\lambda = 780$ nm, continuous wave) passes through the mirror, FSM (Thorlabs-POLARIS-K1S2P, angular resolution is ~0.5 μrad for 0.1 V), HRM (Thorlabs-HRR201-P01), beam splitter (BS_1, T:$R = 90$:10 and BS_3, T:$R = 50$:50), and then enters the next part of the light path. The laser energy enters the detection part at 10% to monitor the positional and angular deviations in real time. The stabilization setup consists of two units: the beam position correction unit (BPCU) and beam angle correction unit (BACU). They work independently to avoid errors caused by the coupling effect of the piezoelectric devices. The second laser beam ($\lambda = 532$ nm, continuous wave) passes through the same optical elements as the first laser.

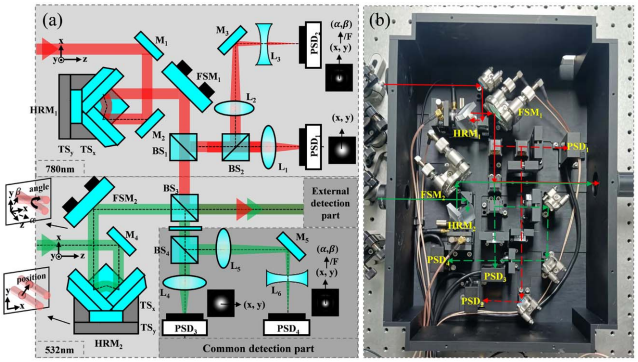

Fig. 2. (a) Schematic of the spatial alignment and stability of multi-beam optical system: M, mirror; TS, translation stage; PSD, position sensitive detector. (b) Experimental setup of the optical system.

Finally, the two beams exit with the same beam center and high stability.

When the system operates, the first laser beam is turned on, and position sensitive detectors, PSD_3 and PSD_4 (Thorlabs-PDQ80A, the resolution is approximately 0.17 μm and the bandwidth is 150 kHz), are used for position and angle detection. The PSD is used as a detector, which has the unique characteristic of being able to accurately monitor the displacement of the incident beam and provides positional information of any spot within the detector region independent of the beam shape, size, or power distribution. HRM_1 and HRM_2 are set on substrates that are connected to two piezo stages (Thorlabs-NF15AP25/M, piezo resolution is 0.76 nm, and response is 1 ms) and can thus move along the x and z directions, which correspond to the x–y plane of the incident plane. Then, by controlling HRM_1 and FSM_1, the beam center position and propagation angle are moved to stable positions that are the same as those of the second laser beam. In addition, the positional information of the beams on PSD_1 and PSD_2 (Thorlabs-PDP90A, the resolution is 0.75 μm, and the bandwidth is 15 kHz) is recorded as the stable parameters of the first laser beam. Subsequently, a filter is placed between BS_3 and BS_4 to block the first laser, and thus only the second laser beam can pass through. Finally, the second laser beam is turned on; PSD_3 and PSD_4 can only detect the second laser beam at this time, and the second laser beam is stabilized at the same position. Through these operations, the two beams can exit with the same beam center and high stability.

The fluctuations can be classified into positional (x, y) and angular (α, β) beam deviations, and a single variable is moved back and forth to compare the designed movement with the actual movement and verify the validity of the parameters and the algorithm. The positional movement ranges from 0 to +5 μm, +5 to −5 μm, and finally back to 0 μm. The angular movement ranges from 0 to +5 μrad, +5 to −5 μrad, and finally back to 0 μrad. Figure 3 shows the results of the single-direction decoupled control experiments. Figures 3(a)–3(d) show the results for the first laser beam and Figs. 3(e)–3(h) for the second laser beam.

Based on these results, we can reach the following conclusions. First, the actual movement coincides well with the

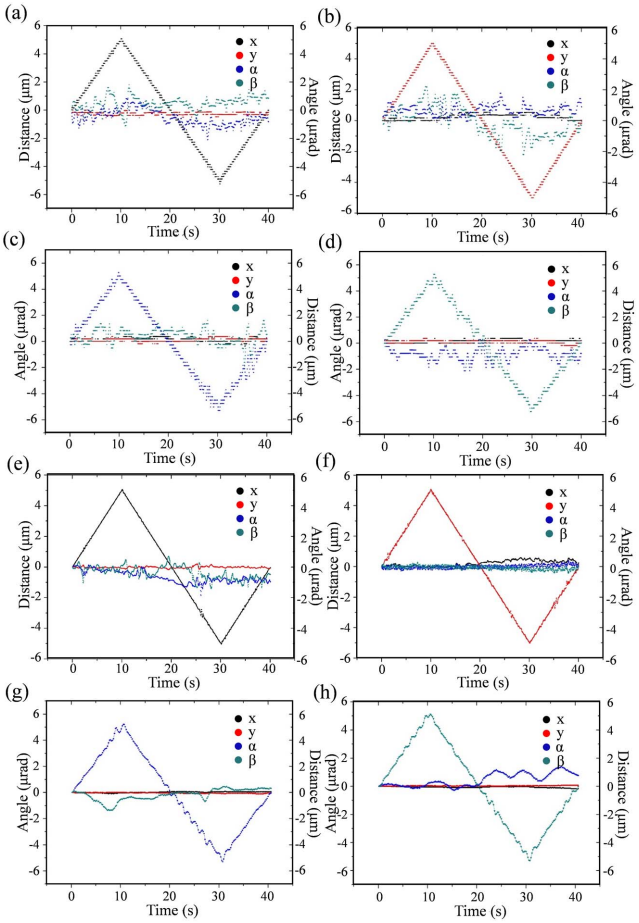

Fig. 3. Single-direction decoupled control results along (a) x, (b) y, (c) α, and (d) β directions of the first laser beam and (e) x, (f) y, (g) α, and (h) β directions of the second laser beam.

designed movement, which indicates the validity of the parameters and algorithm. Second, when one variable changes, the other three variables only change randomly and have nothing to do with the movement of this variable. This means that the system can achieve the regulation of a single variable that avoids errors caused by the coupling effect of piezoelectric devices. Third, the angular deviations of the laser beam are relatively large, which influences the accuracy of the angular correction. However, during the control process, the angular deviations become very small. Finally, the resolution of the detectors used for the first laser beam was smaller than that used for the second laser beam. High-precision detectors were chosen as common detectors to ensure that the two beams were centered, and detectors of a large range were chosen for the first laser beam to increase the adaptability and better align the centers of the two beams.

4. Experimental and Discussion

A scheme based on Fig. 2 was set up in our laboratory to evaluate the performance of the spatial alignment and stability of the multi-beam system. Vortex and solid distributions of the laser beams were selected to observe the coincidence of the beam centers. A CCD (MER-630-60U3C-L) and a lens ($f = 100$ mm) were used to image the two beams, and the spatial alignment was observed in the image results. To further demonstrate the performance of the system, another detector was placed approximately 30 cm from the system to detect the emitted laser beams, as shown in Fig. 4(a).

To better align the centers of the two beams, the position and pointing of the first beam were adjusted through changing the locked positional and angular values. Initially, the positions of the two laser beams were detected, and then the second laser beam was blocked (black arrow), as shown in Fig. 4(b), where the positions of the first laser beam had nearly the same x and y values, indicating that the centers of the two beams overlapped well. The average values of deviations along the x direction were −0.32 and −0.23 μm before and after the second laser beam was blocked, respectively. The relevant average values of deviations along the y direction were 0.30 and 0.43 μm. Therefore, the average errors of center positions along the x and y directions were 0.09 and 0.13 μm, which were equivalent to 0.60 and 0.87 nm at the sample plane under an oil immersion lens ($f = 2$ mm) because the distance between the detector and system was 30 cm.

To test the ability to avoid the errors caused by inaccurate correction calculations and the stability of the system, an active angular disturbance source was added to the first laser beam, as shown in Fig. 5. The detector placed approximately 30 cm from the system showed the results of beam deviation without feedback control [Fig. 5(a)]. The peak-to-valley (PV) value is approximately 30 μm, and the PV value becomes smaller than 1.5 μm with feedback control, as shown in Fig. 5(b).

Figures 6 and 7 show the positional and angular deviations of the first laser beam and the second laser beam, respectively, detected by internal detectors over 1 h with feedback control. The stability of the beam was measured by the STD value, which evaluated the fluctuation of beam drift over much of the time. The deviations along the x and y directions of the first laser beam were, respectively, taken as the abscissa and ordinate of Fig. 6(a), which recorded the position changes of the spot center. The sampling rate of the system was 10 Hz, and the STD values of the deviations were 0.07 and 0.08 μm, respectively. There were intervals between the recording points, which corresponded to the resolution of detectors. We believed the random fluctuations

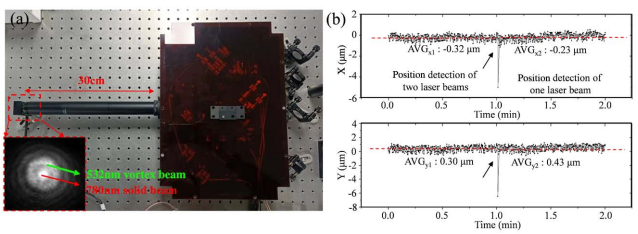

Fig. 4. (a) Photography of the test setup and (b) positional deviations of emitted laser beams detected by external detection. AVG, average.

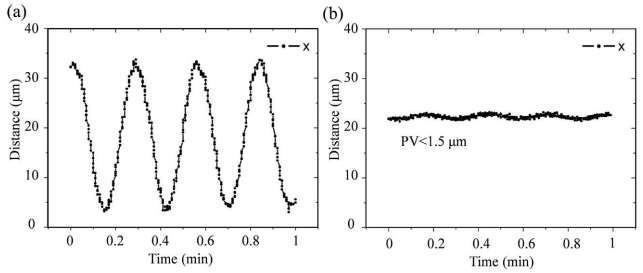

Fig. 5. Under-active disturbance: the results of the external detector (a) without and (b) with feedback for the first laser beam.

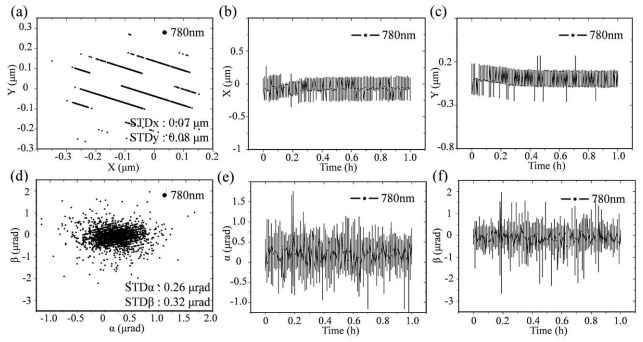

Fig. 6. Display of positional and angular deviations of the first laser beam (780 nm) over 1 h with feedback control. (a) Translational deviations, (b) and (c) deviations along the x and y directions over time, respectively, (d) angular deviations, and (e) and (f) deviations along the α and β directions over time, respectively.

in the results mainly come from the detector's electrical noise. This means that the system control has achieved almost the highest possible accuracy. Figures 6(b) and 6(c) show the variation of the deviations in the x and y directions presented in Fig. 6(a) over time. Despite the obvious random fluctuations, the center remained at essentially the same position. The instantaneous disturbance was found at approximately 0.2 h, and the system could be instantly stabilized, as shown in the figure, which indicates the quick response capability of the system.

The deviations in the α and β directions of the first laser beam were taken as the abscissa and ordinate in Fig. 7(d), respectively, recording the angular changes of the spot center over 1 h. The STD values were 0.26 and 0.32 μrad, respectively, which would cause an error of approximately 0.5 nm at the focal point with an oil immersion lens ($f = 2$ mm). Figures 6(e) and 6(f) show the deviations in the α and β directions simultaneously, as shown in Fig. 6(d). The results showed that the random fluctuations along the angular deviations were larger than those along the positional deviations, which might have been caused by the longer optical path of the angular detection part.

As for the second laser beam, the STD values were 0.03 and 0.04 μm for the positional deviations and 0.65 and 0.57 μrad for the angular deviations, as shown in Figs. 7(a)–7(f). The detection results were the same as those obtained for the first laser beam.

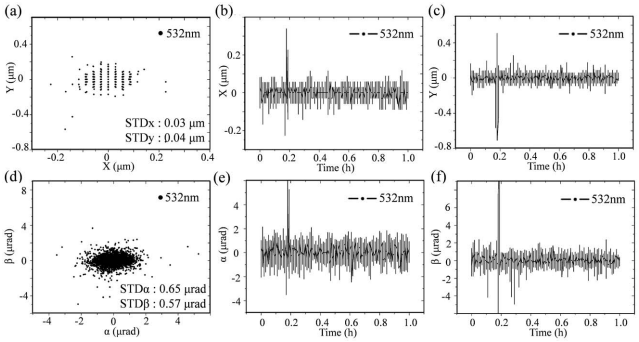

Fig. 7. Display of positional and angular deviations of the second laser beam (532 nm) over 1 h with feedback control. (a) Translational deviations, (b) and (c) deviations along the x and y directions over time, respectively, (d) angular deviations, and (e) and (f) deviations along the α and β directions over time, respectively.

Thus, the error separation technique has advantages for the spatial alignment and stability of beams in multi-beam systems, and the two beams can exit with the same beam center and high stability. With smaller resolution and lower noise of detectors, the spatial alignment and stability of multi-beam optical systems will achieve better performance.

Figure 8 shows the deviations of the incident beams and exit beams over 1 h with feedback control. Two PSDs were placed before our setup to directly detect the deviations before the beams entered the system. The X- and Y-axes drifts of the first laser beam and the second laser beam were over 20 μm, 10 μm and 30 μm, 20 μm, respectively. The laser beams passed through the system of spatial alignment and stability of beams, and a commercial optical beam profiler (DataRay, model: BC2-HR) was placed at the exit to verify the control results. The positional deviations of emitted beams are shown in Fig. 8(c), the sampling rate was 1 Hz, the X- and Y-axes drifts became less than 2 μm, and RMSs were 0.57 and 0.35 μm for x and y directions during 1 h, respectively.

For high-precision optical systems using an objective, angular deviations will have a more serious impact. A lens ($f = 0.30$ m)

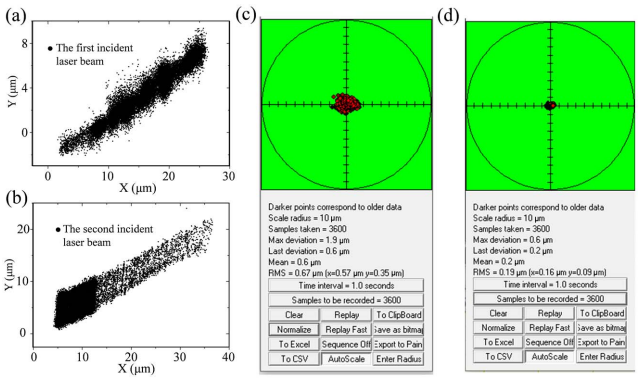

Fig. 8. Deviations of incident laser beams: (a) the first laser beam, (b) the second laser beam, and (c) positional and (d) angular ($f = 0.3$ m) deviations of exit beams under control with an optical beam profiler.

was used with a commercial optical beam profiler to detect the angular deviations of the exit beams. The results of the angular deviations are shown in Fig. 8(d), where the sampling rate was 1 Hz. The X- and Y-axes drifts became less than 0.6 μm, and the RMSs were 0.16 and 0.09 μm for x and y directions over 1 h, respectively. The experimental results showed that the PV values of angular deviations were less than 2 μrad, and the RMSs were approximately 0.53 and 0.30 μrad for the α and β directions, respectively, which were equivalent to approximately 1.06 and 0.60 nm at the sample plane under an oil immersion lens ($f = 2$ mm). The deviations were less than one-third of those currently reported in multi-beam systems in Refs. [17,18].

5. Conclusions

In conclusion, a new method for spatial alignment and stability of beams in a multi-beam system is presented. Compared to previous studies, the error separation technique has the advantage of avoiding alignment errors caused by the coupling effect of piezoelectric devices, inaccurate correction calculation, and detection mode of angular deviation. The spatial alignment and stability of the multi-beam optical system was built with a small size, and the experiments proved that the centers of the two beams overlapped. The average errors of center positions along the x and y directions were 0.09 and 0.13 μm, which were equivalent to 0.60 and 0.87 nm at the sample plane under an oil immersion lens ($f = 2$ mm). The results of internal detectors show that the STD values of the deviations are 0.07 μm, 0.08 μm, 0.26 μrad, and 0.32 μrad for the first laser beam and 0.03 μm, 0.04 μm, 0.65 μrad, and 0.57 μrad for the second laser beam with feedback control. A commercial optical beam profiler was placed at the exit of the system to detect the deviations of the emitted beams, where the positional deviations of exit beams became less than 2 μm, and the RMSs were 0.57 and 0.35 μm for the x and y directions over 1 h, respectively. The angular deviations became less than 2 μrad, and the RMSs were 0.53 and 0.30 μrad for the α and β directions over 1 h, respectively, which were equivalent to approximately 1.06 and 0.60 nm at the sample plane under an oil immersion lens ($f = 2$ mm). The deviations are less than one-third of those currently reported in the relevant literature on multi-beam systems. Although many other factors will affect the precision, such as the temperature fluctuation and external vibration, the results show that the PV values of deviations are close to the resolution of PSDs, which means our system has achieved almost the highest possible accuracy. Thus, with our method, higher alignment and stability accuracy can be achieved to meet the requirement for further development of multi-beam systems, especially those involving high-precision optical systems.

Acknowledgement

This work was supported by the National Key R&D Program of China (No. 2021YFF0502700), National Natural Science Foundation of China (Nos. 52105565 and 62105298), Natural Science Foundation of Zhejiang Province (Nos. LQ22F050015 and LQ22F050017), Postdoctoral Research Foundation of China (No. 2020M671822), Major Scientific Project of Zhejiang Lab (No. 2020MC0AE01), and Major Program of Natural Science Foundation of Zhejiang Province (No. LD21F050002).

References

1. S. W. Hell and J. Wichmann, "Breaking the diffraction resolution limit by stimulated emission: stimulated-emission-depletion fluorescence microscopy," Opt. Lett. **19**, 780 (1994).
2. L. Li, R. R. Gattass, E. Gershgoren, H. Hwang, and J. T. Fourkas, "Achieving $\lambda/20$ resolution by one-color initiation and deactivation of polymerization," Science **324**, 910 (2009).
3. T. F. Scott, B. A. Kowalski, A. C. Sullivan, C. N. Bowman, and R. R. Mcleod, "Two-color single-photon photoinitiation and photoinhibition for subdiffraction photolithography," Science **324**, 913 (2009).
4. P. Müller, R. Müller, L. Hammer, C. Barner-Kowollik, M. Wegener, and E. Blasco, "STED-inspired laser lithography based on photoswitchable spirothiopyran moieties," Chem. Mater. **31**, 1966 (2019).
5. E. Murtezi, S. Puthukodan, B. Buchegger, J. Jacak, and T. A. Klar, "STED controlled photobleaching for sub-diffractional optical nanopatterning," J. Phys. Photonics **2**, 044003 (2020).
6. J. Ma, X. Li, S. Yu, and Q. Han, "Influence of satellite vibration on optical communication performance for intersatellite laser links," Opt. Rev. **19**, 25 (2012).
7. Q. Feng, B. Zhang, and C. Kuang, "A straightness measurement system using a single-mode fiber-coupled laser module," Opt. Laser. Technol. **36**, 279 (2004).
8. M. A. Schwentker, H. Bock, M. Hofmann, S. Jakobs, J. Bewersdorf, C. Eggeling, and S. W. Hell, "Wide-field subdiffraction RESOLFT microscopy using fluorescent protein photoswitching," Microsc. Res. Tech. **70**, 269 (2007).
9. T. J. Gould, D. Burke, J. Bewersdorf, and M. J. Booth, "Adaptive optics enables 3D STED microscopy in aberrating specimens," Opt. Express **20**, 20998 (2012).
10. T. J. Gould, E. B. Kromann, D. Burke, M. J. Booth, and J. Bewersdorf, "Auto-aligning stimulated emission depletion microscope using adaptive optics," Opt. Lett. **38**, 1860 (2013).
11. T. Kanai, A. Suda, S. Bohman, M. Kaku, S. Yamaguchi, and K. Midorikawa, "Pointing stabilization of a high-repetition-rate high-power femtosecond laser for intense few-cycle pulse generation," Appl. Phys. Lett. **92**, 061106 (2008).
12. J. Bao, L. Huang, A. Zeng, B. Ren, B. Yang, X. Peng, and H. Huang, "Study on beam stabilization technique in lithography illumination system," Chin. J. Lasers **39**, 0908004 (2012).
13. S. Liu, S. Tan, Y. Huang, and K. C. Fan, "Design of a compact four degree-of-freedom active compensation system to restrain laser's angular drift and parallel drift," Rev. Sci. Instrum. **90**, 115002 (2019).
14. M. Dobosz, "Interference sensor for ultra-precision measurement of laser beam angular deflection," Rev. Sci. Instrum. **89**, 115003 (2018).
15. B. G. Podlaskin, E. G. Guk, A. G. Obolenskov, and A. A. Sukharev, "Improvement of the accuracy of a position-sensitive detector with a wide field of view," Tech. Phys. Lett. **46**, 988 (2020).
16. S. Chatterjee and Y. P. Kumar, "Measurement of two-dimensional small angle deviation with a prism interferometer," Appl. Opt. **47**, 4900 (2008).
17. Y. Huang, Y. Wang, C. Kuang, and X. Liu, "Method for enhancing stability in multi-beam microscopy," Meas. Sci. Technol. **27**, 105901 (2016).
18. J. Wang, L. Huang, L. Hou, G. He, Q. Song, and H. Huang, "Study of active beam steering system with a simple method," Chin. Opt. Lett. **12**, 081405 (2014).
19. F. Balzarotti, Y. Eilers, K. C. Gwosch, A. H. Gynna, V. Westphal, F. D. Stefani, and S. Hell, "Nanometer resolution imaging and tracking of fluorescent molecules with minimal photon fluxes," Science **355**, 606 (2007).

20. Z. Gan, Y. Cao, R. A. Evans, and M. Gu, "Three-dimensional deep sub-diffraction optical beam lithography with 9 nm feature size," Nat. Commun. **4**, 2061 (2013).
21. C. Ding, D. Zhu, Z. Wei, M. Tang, C. F. Kuang, and X. Liu, "A compact and high-precision method for active beam stabilization system," Opt. Commun. **500**, 127328 (2021).
22. S. Shao, Z. Tian, S. Song, and M. Xu, "Two-degrees-of-freedom piezo-driven fast steering mirror with cross-axis decoupling capability," Rev. Sci. Instrum. **89**, 055003 (2018).
23. E. Csencsics, B. Sitz, and G. Schitter, "Integration of control design and system operation of a high performance piezo-actuated fast steering mirror," IEEE ASME Trans Mechatron. **25**, 239 (2019).